



Published in final edited form as:

Circulation. 2019 May 21; 139(21): 2451–2465. doi:10.1161/CIRCULATIONAHA.118.037357.

## Human Induced Pluripotent Stem Cell Model of Trastuzumab-Induced Cardiac Dysfunction in Breast Cancer Patients

Tomoya Kitani, MD, PhD<sup>1,2,3</sup>, Sang-Ging Ong, PhD<sup>4</sup>, Chi Keung Lam, PhD<sup>1,2,3</sup>, June-Wha Rhee, MD<sup>1,2,3</sup>, Joe Z. Zhang, MD, PhD<sup>1,2,3</sup>, Angelos Oikonomopoulos, PhD<sup>1,2,3</sup>, Ning Ma, PhD<sup>1,2,3</sup>, Lei Tian, PhD<sup>1,2,3</sup>, Jaecheol Lee, PhD<sup>5</sup>, Melinda L. Telli, MD<sup>6</sup>, Ronald M. Witteles, MD<sup>1,3</sup>, Arun Sharma, PhD<sup>7</sup>, Nazish Sayed, MD, PhD<sup>1,2,3</sup>, and Joseph C. Wu, MD, PhD<sup>1,2,3</sup>

<sup>1</sup>Stanford Cardiovascular Institute, Stanford University School of Medicine, Stanford, CA

<sup>2</sup>Institute for Stem Cell Biology and Regenerative Medicine, Stanford University School of Medicine, Stanford, CA

<sup>3</sup>Department of Medicine, Division of Cardiology, Stanford University School of Medicine, Stanford, CA;

<sup>4</sup>Department of Pharmacology and Medicine, University of Illinois College of Medicine, Chicago, IL;

<sup>5</sup>School of Pharmacy, Sungkyunkwan University, Suwon, Republic of Korea;

<sup>6</sup>Department of Medicine, Division of Oncology, Stanford University School of Medicine, Stanford, CA;

<sup>7</sup>Department of Genetics, Harvard Medical School, Boston, MA.

### Abstract

**Background:** Molecular targeted chemotherapies have been shown to significantly improve cancer patient outcomes, but often cause cardiovascular side effects that limit their use and impair patients' quality of life. Cardiac dysfunction induced by these therapies, especially trastuzumab, shows a distinct cardiotoxic clinical phenotype compared to cardiotoxicity induced by conventional chemotherapies.

**Methods:** We employed the human induced pluripotent stem cell-derived cardiomyocyte (iPSC-CM) platform to determine the underlying cellular mechanisms in trastuzumab-induced cardiac dysfunction. We assessed the effects of trastuzumab on structural and functional properties in iPSC-CMs from healthy individuals and performed RNA-sequencing (RNA-seq) to further examine the effect of trastuzumab on iPSC-CMs. We also generated iPSCs from patients receiving trastuzumab and examined whether patients' phenotype could be recapitulated *in vitro* using patient-specific iPSC-CMs.

\*Correspondence: Joseph C. Wu, MD, PhD, 265 Campus Drive, Rm G1120B, Stanford, CA 94305-5454, Tel: (650) 736-2246. joewu@stanford.edu or Nazish Sayed, MD, PhD, 300 Pasteur Drive, Grant Building S114, Stanford, CA 94305-5454. Tel: (650) 736-2863. sayedns@stanford.edu.

DISCLOSURES

None

**Results:** We found that clinically relevant doses of trastuzumab significantly impaired the contractile and calcium handling properties of iPSC-CMs without inducing cardiomyocyte death or sarcomeric disorganization. RNA-seq and subsequent functional analysis revealed mitochondrial dysfunction and altered cardiac energy metabolism pathway as primary causes of trastuzumab-induced cardiotoxic phenotype. Human iPSC-CMs generated from patients who received trastuzumab and experienced severe cardiac dysfunction were more vulnerable to trastuzumab treatment, compared to iPSC-CMs generated from patients who did not experience cardiac dysfunction following trastuzumab therapy. Importantly, metabolic modulation with AMPK activators could avert the adverse effects induced by trastuzumab.

**Conclusion:** Our results indicate that alterations in cellular metabolic pathways in cardiomyocytes could be a key mechanism underlying the development of cardiac dysfunction following trastuzumab therapy; therefore, targeting the altered metabolism may be a promising therapeutic approach for trastuzumab-induced cardiac dysfunction.

### Keywords

heart failure; cardiotoxicity

## INTRODUCTION

Cardiovascular complications of cancer therapy are the leading cause of morbidity and mortality in cancer survivors and limit the clinical use of various chemotherapeutic agents<sup>1–3</sup>. The successful development of modern cancer therapy has dramatically improved patient outcome in many cancer types, but some anti-cancer therapeutics can lead to myocardial injury and vascular endothelial dysfunction, resulting in cardiovascular events such as hypertension, arrhythmia, thromboembolism, and heart failure<sup>4</sup>. One of the most serious cardiovascular adverse effects of chemotherapy is the development of left ventricular dysfunction, which is typically detected as reduced left ventricular ejection fraction that significantly interferes with optimal therapy and quality of life for patients. There is growing evidence that novel molecular targeted anti-cancer agents cause distinct patterns of cardiac dysfunction compared to those from a traditional class of anti-cancer agents (e.g., anthracyclines)<sup>5</sup>. Although the use of a variety of molecular targeted drugs has been implicated in cardiac dysfunction, the most frequent occurrence has been reported in association with trastuzumab (Herceptin), a humanized monoclonal antibody against human epidermal growth factor receptor 2 (HER2)<sup>6</sup>.

HER2 is a well-known proto-oncogene found especially upregulated in breast cancer. The HER2 signaling pathway can be activated independently by exogenous factors via dimerization or through neuregulin-1 released from endothelial cells, which induces cell growth, division, angiogenesis, survival, and migration; therefore the activation of HER2 signaling plays an important role in the pathogenesis of some cancers<sup>7</sup>. Indeed, trastuzumab therapy has been shown to significantly improve clinical outcomes among patients with HER2-positive cancer by inhibiting tumor growth and inducing immune system-mediated cancer cell death<sup>8</sup>. HER2 signaling also plays a vital role in the development and function of the heart<sup>9, 10</sup>. Previous studies suggested that inhibition of HER2 signaling could increase the vulnerability of the heart to stress derived from aging and pressure overload, resulting in

loss of cardiomyocyte viability<sup>11, 12</sup>. However, these results are not yet sufficient to explain the mechanism underlying trastuzumab-induced cardiac dysfunction, as numerous clinical studies have reported reversible myocardial injury without apparent structural damage in most patients<sup>5</sup>.

Over the last decade, human induced pluripotent stem cell-derived cardiomyocytes (iPSC-CMs) have proven to be an ideal platform for studying human cardiovascular disease with great success in modeling many types of genetic cardiac diseases, including cardiac channelopathies, cardiomyopathies, developmental heart defects, and inherited metabolic disorders<sup>13, 14</sup>. In addition, iPSC-CMs have also been shown to be capable of modeling other types of cardiac diseases in which the underlying genetic causes are not yet clear, including viral myocarditis caused by the B3 strain of coxsackievirus<sup>15, 16</sup>, doxorubicin-induced cardiotoxicity<sup>17</sup>, and diabetic cardiomyopathy<sup>18</sup>, thereby highlighting their usefulness as a general platform for studying a wide range of cardiovascular diseases. Recently, we showed that iPSC-CMs can be used to assess the cardiac toxicity induced by multiple tyrosine kinase inhibitors<sup>19</sup>. Therefore, investigating the mechanisms of disease pathogenesis and therapeutic interventions using human iPSC-CMs may provide useful insights that could lead to the development of new therapeutic interventions.

Here we used human iPSC-CMs generated from healthy individuals and patients receiving trastuzumab to investigate the mechanism of trastuzumab-induced cardiac dysfunction. We demonstrate that treatment of iPSC-CMs with trastuzumab can recapitulate the clinical features exhibited by patients. Transcriptome analysis revealed the key role of an altered energy metabolism pathway for cardiomyocytes in disease pathogenesis. Furthermore, we also found that iPSC-CMs generated from patients developing severe cardiac dysfunction following trastuzumab therapy are more vulnerable to trastuzumab treatment. Finally, we found that the use of metabolic modulators could serve as a potential therapy for treating trastuzumab-induced cardiac dysfunction.

## METHODS

An extended methods section is available in the Supplementary Materials. All data, methods used in the analysis, and study materials for the purposes of reproducing the results or replicating procedures can be made available upon request to the corresponding author.

### Study design.

To investigate the molecular mechanisms underlying trastuzumab-induced cardiac dysfunction, three control iPSC-CMs were treated with trastuzumab or doxorubicin for 7 days. For generation of patient-specific iPSC lines, we recruited breast cancer patients who had been treated with trastuzumab therapy at Stanford University Medical Center, including patients clinically diagnosed with trastuzumab-induced cardiac dysfunction and patients who did not experience cardiac side effect with at least 1-year trastuzumab therapy. A minimum of two biological replicates were performed in each iPSC line for each experiment, with the exception of RNA-seq experiments.

### Derivation and culture of human iPSCs.

Three control human iPSC lines from healthy individuals (SCVI-114, SCVI-116, and SCVI-273) were obtained from Stanford Cardiovascular Institute iPSC Biobank. Sendai viral reprogramming was used to generate all human iPSC lines from peripheral blood mononuclear cells obtained from individuals who gave informed consent under protocols approved by the Stanford University Human Subjects Research Institutional Review Board as described previously<sup>20</sup>. Human iPSCs were grown on Matrigel-coated (Corning) plates using chemically defined E8 medium (Thermo Fischer Scientific) and passaged at a 1:12 ratio every four days using Accutase solution (Sigma-Aldrich).

### Cardiac differentiation of human iPSCs.

Human iPSC lines were differentiated into iPSC-CMs using a small molecule-based monolayer differentiation protocol and were maintained as previously published<sup>21</sup>. Briefly, iPSC monolayers were cultured to 85% cell confluency and were then differentiated into cardiomyocytes with 6  $\mu\text{mol/L}$  CHIR99021 (Selleck Chemicals) in RPMI plus B27 without insulin (Thermo Fisher Scientific) (days 0–1), followed by 5  $\mu\text{mol/L}$  IWR-1 (Sigma-Aldrich) for 48 hours (days 3–4). On day 10, cells were glucose-starved for 5 days with RPMI without D-glucose plus B27 to purify cardiomyocytes. After purification, cells were cultured in RPMI plus B27. When replating iPSC-CMs for downstream use, cells were dissociated with Accutase solution (Sigma-Aldrich) into a single-cell suspension and seeded on Matrigel-coated plates at a density of 120,000 cells/cm<sup>2</sup>.

### Drug treatment.

Trastuzumab was kindly provided by Genentech Inc. (MTA OR-215366). Human iPSC-CMs were treated with trastuzumab or doxorubicin (Sigma-Aldrich) for 7 days. Human IgG (Sigma Aldrich) was used as a control treatment unless noted. For the co-treatment experiment, cells were treated with AICAR (Sigma-Aldrich), rosiglitazone (Thermo Fisher Scientific), metformin (Sigma-Aldrich), or lipoic acid (Cayman Chemical) at 0.001 to 1 mM, or rapamycin (Sigma-Aldrich) at 0.001 to 1  $\mu\text{M}$  in the presence of trastuzumab at 1  $\mu\text{M}$  for 7 days. The medium containing fresh drug was replaced every 3 days.

### Contractility analysis.

Dissociated iPSC-CMs were seeded on Matrigel-coated 96-well plates and cultured for 7 days to recover their spontaneous beating before the assay. Spontaneous beating activity of monolayer cardiomyocytes were recorded with high resolution motion capture tracking using the SI8000 Live Cell Motion Imaging System (Sony Corporation). During data collection, cells were maintained under controlled humidified conditions at 37 °C with 5% CO<sub>2</sub> and 95% air in a stage-top microscope incubator (Tokai Hit). Functional parameters were assessed from the averaged contraction-relaxation waveforms during a 10-second recording before starting drug treatment (baseline) and after 7 days of drug treatment. All post-drug assessments were normalized to their respective baseline values. Further details on the motion vector analysis are provided in the Supplementary Materials.

### Quantitative plate-based assays.

Human iPSC-CMs plated on 96-well plates were subjected to plate-based assays after 7 days of drug treatment using a Cytation 5 plate reader/imager (BioTek Instruments). PrestoBlue (Life Technologies) was used for cellular viability assay, CYTO-ID Autophagy detection kit 2.0 (Enzo Life Sciences) was used for autophagy assay, JC-10 (Enzo Life Sciences) was used for mitochondrial membrane potential measurement, ROS-Glo H<sub>2</sub>O<sub>2</sub> (Promega) was used for ROS detection, and Cell Titer Glo (Promega) was used for ATP content assay. For measurement of troponin I and glucose levels in cell culture media, day 6–7 media were collected during 7 days of drug treatment and centrifuged to remove dead cells. Troponin I and glucose concentrations in the supernatant were measured by using the Glucose Colorimetric/Fluorometric Assay Kit (BioVision) and Human Cardiac Troponin I ELISA kit (RayBiotech), respectively. All assays were performed according to the manufacturer's instructions.

### Statistical analysis.

All data are expressed as mean  $\pm$  SEM unless otherwise specified. Statistical comparisons were performed using one-way ANOVA followed by the Holm–Sidak multiple comparisons test, or the two-tailed Student's t-test using GraphPad Prism 7. Values of  $P < 0.05$  were considered to be statistically significant (NS, not significant; \*,  $P < 0.05$ ; \*\*,  $P < 0.01$ ).

## RESULTS

### Recapitulating the clinical phenotype of trastuzumab-induced cardiac dysfunction with iPSC-CMs

To investigate whether iPSC-CMs can recapitulate the disease phenotype of trastuzumab-induced cardiac dysfunction, we began by examining the effects of trastuzumab treatment in iPSC-CMs from three healthy individuals (Fig. S1A). Human iPSC-CMs were differentiated using a monolayer-based cardiac differentiation protocol, and the cells were then glucose-starved to increase the purity of cardiomyocytes (Fig. S1B–C). All iPSC-CMs exhibited spontaneous beating after day 15 of differentiation. Phosphorylation of HER2 and HER4, expressed in adult cardiomyocytes<sup>22</sup>, was confirmed in iPSC-CMs by receptor tyrosine kinase phosphorylation arrays (Fig. S1D). Human iPSC-CMs of 30–35 days post-differentiation were exposed to a clinical dose of trastuzumab (0.1 to 1  $\mu$ M) or a low dose of doxorubicin (0.05 and 0.1  $\mu$ M) for 7 days, and the cells were then subjected to downstream assays (Fig. 1A).

Given that clinical studies have shown no significant structural changes in patients' myocardium despite having marked reduction in ventricular ejection fraction during trastuzumab therapy<sup>5</sup>, we assessed the effects of drug treatment on cell viability of human iPSC-CMs using a fluorescence-based resazurin assay. In contrast to doxorubicin, we found that trastuzumab did not reduce cell viability after 7 days of treatment (Fig. 1B). Similarly, immunostaining for sarcomere assembly using anti-cardiac troponin T and anti- $\alpha$ -actinin antibody revealed no sarcomere disarray with trastuzumab when compared to doxorubicin that showed increased sarcomeric disarray (Fig. 1C–D). Next, we measured the level of released cardiac troponin I, a biomarker of cardiomyocyte injury, in the cell culture medium,

and observed no significant increase in troponin I after trastuzumab treatment (Fig. 1E), which is consistent with the interpretation that trastuzumab alone does not cause irreversible damage in cardiomyocytes.

We next assessed the effect of drug treatment on the contractile properties of human iPSC-CMs using high-speed video microscopy with motion vector analysis (Fig. S2A)<sup>23, 24</sup>. Strikingly, we observed a significant decrease in contraction velocity and deformation distance of monolayer iPSC-CMs with no changes in the spontaneous beating rate and contraction-relaxation duration after trastuzumab treatment (Fig. 1F–H and S2B–C). The relaxation velocity of iPSC-CMs also showed a decreasing trend but did not reach statistical significance (Fig. S2D). We next performed calcium imaging measurement at the single cell level in iPSC-CMs using the fluorescent indicator Fura-2. Consistent with the impairment in contractility, we found that trastuzumab decreased calcium amplitude and prolonged calcium removal in iPSC-CMs in a similar manner to doxorubicin (Fig. 1I–K). Taken together, these results demonstrated that human iPSC-CMs treated with trastuzumab can recapitulate clinical phenotypes of trastuzumab-treated patients, characterized by contractile dysfunction in the absence of cell death and sarcomeric structural abnormalities.

### Transcriptomic analysis of the effect of trastuzumab in human iPSC-CMs

To examine the mechanisms associated with contractile dysfunction in iPSC-CMs following trastuzumab treatment, we next performed RNA-seq on iPSC-CMs after 7 days of trastuzumab treatment. Principal component analysis (PCA) of all expressed transcripts revealed substantial differences between trastuzumab-treated and untreated control groups among all three iPSC-CM lines (Fig. 2A). Moreover, hierarchical clustering of gene expression profiles under statistical analysis (false discovery rate (FDR) < 0.1 and fold-change > 1.5) showed distinct patterns of gene expression between trastuzumab treated and untreated control groups (Fig. 2B). We then used Ingenuity Pathway Analysis (IPA) to further explore the biological significance of differently expressed genes obtained from the above process. Notably, the canonical pathway analysis in IPA revealed a high enrichment of pathways involved in mitochondrial dysfunction and oxidative phosphorylation (Fig. 2C), suggesting their possible role in the pathogenesis of trastuzumab-induced cardiac dysfunction. We next performed toxicology analysis using IPA, which revealed that cardiac dilatation, cardiac dysfunction, and cardiac enlargement were ranked in the top five of toxicity functions predicted from the gene expression patterns induced by trastuzumab treatment (Fig. 2D), validating that our *in vitro* model system with human iPSC-CMs can be effectively used to study the disease mechanisms in patients with trastuzumab-induced cardiac dysfunction.

### Disturbed mitochondrial function in iPSC-CMs following trastuzumab treatment

As our canonical pathway analysis of the transcriptome data (Fig. 2C) indicated that mitochondrial dysfunction and oxidative phosphorylation play a key role in the pathogenesis of trastuzumab-induced cardiac dysfunction, we next examined the changes in mitochondrial function and biogenesis in iPSC-CMs after 7 days of drug treatment (Fig. 3A). Quantification of mitochondrial membrane potential ( $\Psi_m$ ) using the JC-10 probe demonstrated that  $\Psi_m$  was minimally affected by trastuzumab treatment, whereas



doxorubicin significantly reduced  $\Psi_m$  in iPSC-CMs (Fig. 3B). We also measured the rate of reactive oxygen species (ROS) generation following treatment and found no clear differences between the trastuzumab-treated and untreated control groups (Fig. S3A–B). These results are consistent with our previous results showing that cardiomyocyte death is not observed after trastuzumab treatment (Fig. 1B and 1E). Next, we evaluated the mitochondrial respiratory function with a mitochondrial stress test using the Seahorse XF96 extracellular-flux analyzer. Notably, we observed significant reductions in basal, maximal, and ATP-linked respiration in iPSC-CMs after trastuzumab treatment (Fig. 3C–D). We also observed a decrease in cellular ATP content in iPSC-CMs following trastuzumab treatment (Fig. S3C). Furthermore, we quantified the relative mitochondrial DNA copy number, which was significantly decreased after treatment with trastuzumab or doxorubicin (Fig. 3E). Consistent with this finding, the protein amount of oxidative phosphorylation (OXPHOS) complexes as assessed by immunoblotting was also decreased by treatment with trastuzumab or doxorubicin (Fig. 3F–3G). Taken together, these results suggest that disturbed mitochondrial function is a key player in trastuzumab-induced cardiac dysfunction.

### Changes in energy metabolism pathway in iPSC-CMs induced by trastuzumab

To gain more insight into the mechanism of trastuzumab-induced cardiac dysfunction, we next performed an upstream regulator analysis of altered expressed genes identified by RNA-seq in iPSC-CMs following trastuzumab treatment (Fig. S4A–B). We conducted an interaction analysis of the upstream regulators using STRING. We found that several key genes involved in cardiac energy metabolism were dysregulated in iPSC-CMs following trastuzumab treatment, including INSR/IGF1R, mTOR, and PGC1 $\alpha$  (Fig. 4A). To probe these changes in the signaling pathways in iPSC-CMs, we assessed the changes in the phosphorylation status of intracellular signaling kinases induced by trastuzumab treatment using a human phospho-kinase array. Consistent with the results in the upstream regulator analysis, we observed substantial changes in the phosphorylation state of key proteins related to cardiac energy metabolism, including AKT (S308, S473), S6K1 (T389), mTOR (S2448), STAT3 (S727), and AMPK $\alpha$ 1/2 (T183/172) (Fig. 4B and S5A). Similar findings were also obtained using Western blot analysis (Fig. S5B–C). As macroautophagy (hereafter briefly referred to as autophagy) is a critical process for maintaining cellular energy homeostasis that is affected by changes in cellular metabolic status<sup>25</sup>, we evaluated autophagic activity and observed decreased autophagy levels in iPSC-CMs following trastuzumab treatment, supporting the likelihood of changes in intracellular energy status (Fig. 4C and S6A–B). To further confirm the changes in energy metabolism, we measured the glucose concentration of the cell culture medium and found that glucose uptake was significantly reduced in iPSC-CMs following trastuzumab treatment (Fig. 4D).

Based on previous studies that suggested the importance of myocardial energy metabolism in heart function<sup>26</sup>, we hypothesized that altered energy metabolism in cardiomyocytes could contribute to the development of trastuzumab-induced cardiac dysfunction. To test this hypothesis, we examined whether the detrimental effects of trastuzumab in iPSC-CMs could be ameliorated by modulating energy metabolism with the co-treatment of 5-amino-4-imidazolecarboxamide riboside (AICAR), a pharmacological activator of AMP-activated

protein kinase (AMPK). AMPK is considered a central regulator of cellular energy homeostasis, and its activation is emerging as a potential therapeutic target for various metabolic disorders in humans<sup>27</sup>. In addition, AMPK activation has been reported to increase muscle glucose uptake<sup>28</sup>. As expected, we found that AICAR treatment attenuated trastuzumab-induced reduction of glucose uptake in iPSC-CMs (Fig. 4D). AICAR treatment did not induce conduction slowing associated with a significant risk of drug-induced fatal arrhythmias in iPSC-CMs (Fig. S7A–B). We next evaluated the protective effect of AICAR treatment on trastuzumab-induced mitochondrial dysfunction using the mitochondrial stress test. We observed that AICAR treatment ameliorated the impaired mitochondrial respiratory capacity induced by trastuzumab in iPSC-CMs (Fig. 4E). Finally, we tested the protective effect of AICAR treatment on contraction dysfunction in iPSC-CMs induced by trastuzumab and found that AICAR treatment resulted in an improvement of contraction velocity and deformation distance suppressed by trastuzumab (Fig. 4F and S7C–E). These results suggest that altered energy metabolism pathways in cardiomyocytes play a vital role in the development of trastuzumab-induced cardiac dysfunction.

### Recapitulation of patient-specific responses to trastuzumab therapy in iPSC-CMs

Next, we generated iPSCs from seven breast cancer patients previously treated with trastuzumab therapy, including five patients clinically diagnosed with trastuzumab-induced cardiac dysfunction without concurrent anthracycline chemotherapy or concomitant cardiovascular disease. We classified the recruited patients into the following three subgroups: non-toxic patient (NP, no cardiac side effect for at least 1-year treatment with trastuzumab), moderately toxic patients (MP, LVEF decline < 20% to less than 55%), and severely toxic patients (SP, LVEF decline 20% to less than 55%) (Fig. S8A–C). To test whether human iPSC-CMs can recapitulate the patient-specific response to trastuzumab therapy, we assessed the effect of trastuzumab in patient-specific iPSC-CMs (Fig. 5A–B). Consistent with our previous data, trastuzumab treatment on all patient-specific iPSC-CMs showed no reduction in cell viability (Fig. 5C).

We next assessed the effect of trastuzumab on contractile properties of patient-specific iPSC-CMs. Interestingly, the trastuzumab treatment significantly reduced the contraction velocity and deformation distance in the SP group compared to the NP or MP group (Fig. 5D–E and S9A–D). Similarly, the mitochondrial stress test showed a significant decrease in the mitochondrial respiratory capacity following trastuzumab treatment in the SP group compared to the NP group (Fig. 5F). Furthermore, we observed that trastuzumab treatment reduced glucose uptake and autophagic activity of iPSC-CMs to a greater extent in the SP group than the NP group (Fig. 5G–H). Taken together, these data demonstrate that iPSC-CMs can recapitulate patient-specific response to trastuzumab therapy.

### Drug testing for trastuzumab-induced cardiac dysfunction using iPSC-CMs

Finally, to test the therapeutic potential of targeting the energy metabolism pathway, we used iPSC-CMs generated from the most severely toxic patient (SP1) to assess the changes in contractile properties following co-treatment with trastuzumab and respective therapeutic candidate agents (Fig. 6A). Given our observation that AICAR ameliorates cardiomyocyte dysfunction induced by trastuzumab in iPSC-CMs from healthy individuals, we selected



several drugs in current use that are known to increase AMPK activity, including metformin, rosiglitazone, resveratrol, and lipoic acid<sup>29</sup>. Additionally, we included the mTOR inhibitor rapamycin to determine whether suppressing the mTOR signaling pathway, which was found to be upregulated by trastuzumab, can ameliorate trastuzumab-induced cardiomyocyte dysfunction. Notably, we observed that the reduction of contraction velocity following trastuzumab treatment was rescued by co-treatment with all tested drugs by enhancing AMPK activity at optimal concentrations (Fig. 6B). In contrast, rapamycin failed to overcome the effects of trastuzumab, suggesting that pleiotropic effects of AMPK on cellular metabolism may be required to restore the impaired cardiac function induced by trastuzumab (Fig. 6B and S10A). Consistent with these findings, rapamycin treatment also failed to rescue the reduced cellular ATP levels despite improving glucose uptake (Fig. S10B–C). Taken together, these results indicate that targeting the altered energy metabolism pathway could serve as a potential approach to prevent and manage cardiac dysfunction induced by trastuzumab therapy in cancer patients.

## DISCUSSION

Due to the global rising burden of cancer and cardiovascular disease, cardiovascular side effects of cancer therapies have become a significant clinical problem<sup>1, 2</sup>. Notwithstanding continuing efforts to minimize the toxic side effects of cancer treatments, modern targeted cancer therapies can provoke cardiac dysfunction exhibiting distinct clinical features from conventional chemotherapy-induced cardiotoxicity<sup>5</sup>. Despite these complications, there is no effective treatment for these patients except for withdrawal of the drug, and elucidation of the pathogenic mechanisms has been hampered by the antigenic specificity against human cells<sup>6</sup>.

In this study, we showed that the human iPSC-CM model can recapitulate the clinical phenotype of trastuzumab-induced cardiac dysfunction and further elucidated that altered energy metabolism pathways underlie the mechanism of impaired cardiac function. We successfully demonstrated that restoring the impaired energy metabolism with AMPK activation can attenuate cardiomyocyte dysfunction following trastuzumab treatment. We also showed that human iPSC-CMs can recapitulate patient-specific vulnerability to cardiac dysfunction induced by trastuzumab therapy. Furthermore, human iPSC-CMs generated from patients with the most severe cardiac dysfunction were used to test therapeutic candidates for treating trastuzumab-induced cardiac dysfunction.

The HER2 signaling pathway has been shown to be important in regulating normal heart development and stress response of the heart<sup>9, 10, 30, 31</sup>. Therefore, the inhibition of HER2 signaling pathway seems to provide a plausible explanation for cardiac dysfunction in patients after trastuzumab treatment. However, its underlying molecular mechanism is poorly understood, and important questions remain unanswered. For example, previous studies showed that blockade of HER2 signaling pathway induced cardiomyocyte death via ROS production, leading to myocardial damage in rodent model and isolated human cardiomyocytes<sup>32–36</sup>. However, its reversibility upon drug withdrawal in the clinical setting is unlikely to be explained by permanent damage to the myocardium. In addition, cardiac biopsy specimens from patients with trastuzumab-induced cardiac dysfunction typically do

not show structural changes in the myocardium such as myocyte destruction<sup>5</sup>, which is characteristic of anthracycline-induced cardiotoxicity. Indeed, all patients with trastuzumab-induced cardiac dysfunction in our study recovered cardiac function to near baseline levels after drug withdrawal (Fig. S8B). In our experiments, we did not observe any evidence of cardiomyocyte death after 7 days of trastuzumab treatment in iPSC-CMs derived from 10 individuals, including 5 patients who were clinically diagnosed with trastuzumab-induced cardiac dysfunction, which shows that the *in vitro* iPSC-CM model can recapitulate key features of trastuzumab-induced cardiac dysfunction in patients.

Myocardial contractile dysfunction is a characteristic feature of patients with trastuzumab-induced cardiac dysfunction. In this study, we observed a decrease in the maximum speed of motion during the contraction phase (contraction velocity) and in the overall deformation of motion during the contraction-relaxation process (deformation distance) in monolayer iPSC-CMs. Although high-speed video microscopy with motion vector analysis allows us to evaluate the changes in the contractile properties of iPSC-CMs in a label-free and non-invasive manner, one limitation in this approach is the lack of evaluation of electrophysiological properties. Nevertheless, we did not find significant changes in electrical propagation speed in monolayer iPSC-CMs using the MEA system. In addition, we observed that trastuzumab treatment impairs calcium handling properties at the single-cell level in iPSC-CMs without exerting a significant effect on contraction-relaxation duration in motion vector analysis. Altogether, these findings indicate that impaired electrical coupling between cardiomyocytes is not a major contributor to the reduced contraction velocity and deformation distance observed in motion vector analysis with trastuzumab treatment. This conclusion is also supported by the clinical observation that malignant ventricular arrhythmias are rarely reported and usually secondary to systolic dysfunction in patients with trastuzumab-induced cardiac dysfunction.

Alterations in cardiac energy metabolism are a key feature of heart failure and are thought to contribute to its progression<sup>26</sup>. Although details of the alteration in energy metabolism vary depending on the etiology and stage of heart failure, mitochondrial dysfunction is recognized as an essential contributor to cellular dysfunction. We found that trastuzumab induced mitochondrial dysfunction and changed the energy metabolism pathway in iPSC-CMs, including by activating of the mTOR signaling pathway. Additionally, we observed decreased glucose uptake and reduced autophagic activity in iPSC-CMs following trastuzumab treatment, which is consistent with previous studies<sup>37, 38</sup> and supportive of the hypothesis that trastuzumab affects the energy metabolic status in cardiomyocytes. Interestingly, similar patterns of changes in cardiac energy metabolism also have been shown in the pathogenesis of diabetes-induced cardiac dysfunction known as diabetic cardiomyopathy (DbCM)<sup>39</sup>. Although the precise mechanism of DbCM is still a subject of debate, activation of AMPK has been shown to regulate metabolism and restore cardiac function in DbCM by activating autophagy and promoting glucose metabolism<sup>39</sup>. Indeed, we observed that the AMPK activator, AICAR, attenuated mitochondrial dysfunction and contractile dysfunction induced by trastuzumab in iPSC-CMs, suggesting that alterations in energy metabolism may play a key role in trastuzumab-induced cardiac dysfunction.

In recent years, patient-specific iPSC models have provided powerful platforms to study diverse human diseases, including cardiovascular disease. Differentiated cells from iPSCs still exhibit relatively immature phenotypes and have difficulty simulating individual environments or epigenetic alterations. Nevertheless, patient-specific iPSC-CMs are emerging as a promising option to calculate individual disease susceptibility and drug response for cardiovascular precision medicine because they can provide human cardiomyocytes carrying any given individual's genetic makeup, including any potential genetic variants associated with the relevant disease and drug response<sup>14</sup>. We enrolled patients without clear risk factors for trastuzumab-induced cardiac dysfunction (e.g., concurrent use of anthracyclines or concomitant cardiovascular disease) and observed that patient-specific iPSC-CMs displayed a more severe phenotype following trastuzumab treatment in the SP group than in the MP or the NP group, suggesting that patients in the SP group may possess combinations of genetic variants associated with increased vulnerability to trastuzumab-induced cardiac dysfunction. Building on previous studies<sup>17, 40</sup>, our results provide further support for the use of patient-specific iPSC-CMs to predict individual risks of drug induced-cardiotoxicity.

There is growing evidence suggesting that conventional medications for patients with heart failure, such as  $\beta$ -blockers or renin-angiotensin inhibitors, may be cardioprotective in chemotherapy-induced cardiac dysfunction<sup>41–43</sup>. However, their clinical applicability for trastuzumab-induced cardiac dysfunction is limited due to the small sample sizes of relevant clinical trials and the fact that most of the studies have focused on anthracycline-induced cardiac dysfunction. Given that AMPK is well recognized as a key regulatory kinase in myocardial energy metabolism and that metabolic alterations are observed in the failing heart, pharmacological activation of AMPK has been tested to treat some types of heart diseases<sup>44, 45</sup>. For example, metformin may improve cardiac function after myocardial infarction<sup>46, 47</sup>. Although a randomized clinical trial failed to confirm any cardioprotective effect from the acute administration of metformin in non-diabetic myocardial infarction patients, numerous other experimental studies have shown beneficial effects of chronic metformin treatment in ischemic myocardium, especially in the context of metabolic syndrome, supporting the idea that pharmacological intervention targeting cellular energy metabolism could be cardioprotective in some disease settings<sup>48, 49</sup>. Notably, activation of AMPK has been reported to suppress tumor progression and increase sensitivity to chemotherapy and radiotherapy in various cancers, including breast cancer<sup>27</sup>. Therefore, it is clinically appropriate to investigate whether AMPK activators could be used for prevention or treatment of trastuzumab-induced cardiac dysfunction in cancer patients. To that end, we found that the AMPK activator, AICAR, can ameliorate mitochondrial dysfunction and contractile dysfunction induced by trastuzumab in iPSC-CMs from healthy individuals. To extend this finding, we further tested AMPK activators in our *in vitro* model of trastuzumab-induced cardiac dysfunction using iPSC-CMs derived from the most severely toxic patient to identify potential therapeutic interventions.

Our results showed that mTOR inhibition by rapamycin did not improve the contraction velocity impaired by trastuzumab. In agreement with these observations, accumulating evidence demonstrates that AMPK activation not only inhibits mTORC1 signaling via direct phosphorylation of RAPTOR, a key component within mTORC1 complex, but also directly

activates unc-51-like autophagy-activating kinase 1/2 (ULK1/2), which also plays a key role in regulating cellular energy metabolism. Moreover, both AMPK and mTORC1 are also regulated by ULK1 through feedback circuits<sup>50</sup>. Collectively, our results demonstrate the need to further investigate these complex interactions to target myocardial energy metabolism for the treatment of cardiovascular diseases.

In summary, we used human iPSC-CMs from healthy individuals and patients with cardiac dysfunction during trastuzumab therapy, and showed that trastuzumab induces cellular dysfunction in iPSC-CMs that is distinct from the classical chemotherapy-induced cardiotoxicity resulting in cardiomyocyte death (Fig. 6C). Our results suggest that altered energy metabolism pathways underlie the cardiomyocyte dysfunction during trastuzumab therapy, and therefore targeting the energy metabolism pathway may be a new approach to mitigate the cardiac side effects of trastuzumab therapy in cancer patients.

## Supplementary Material

Refer to Web version on PubMed Central for supplementary material.

## ACKNOWLEDGEMENTS

We would like to thank Blake Wu for editing the manuscript. We thank Andrew Olson from Stanford Neuroscience Microscopy Service (NMS) for help with confocal imaging.

### SOURCES OF FUNDING

This study was funded by the National Institutes of Health (NIH) grants R01 HL123968, R01 HL128170, R01 HL141851, and R01 HL132875 (J.C.W.), Japan Heart Foundation/Bayer Yakuhin Research Grant Abroad (T.K.), American Heart Association 18POST33960304 (N.M.), NIH K01 HL135455, and Stanford Translational Research and Applied Medicine (TRAM) pilot grant (N.S.).

## REFERENCES

1. Ewer MS and Ewer SM. Cardiotoxicity of anticancer treatments. *Nat Rev Cardiol.* 2015;12:547–558. [PubMed: 25962976]
2. Lenneman CG and Sawyer DB. Cardio-oncology: an update on cardiotoxicity of cancer-related treatment. *Circ Res.* 2016;118:1008–1020. [PubMed: 26987914]
3. Chang HM, Moudgil R, Scarabelli T, Okwuosa TM and Yeh ETH. Cardiovascular complications of cancer therapy: best practices in diagnosis, prevention, and management: part 1. *J Am Coll Cardiol.* 2017;70:2536–2551. [PubMed: 29145954]
4. Stack JP, Moslehi J, Sayed N and Wu JC. Cancer therapy-induced cardiomyopathy: can human induced pluripotent stem cell modelling help prevent it? *Eur Heart J.* 2018;10.1093/eurheartj/ehx811.
5. Ewer MS and Lippman SM. Type II chemotherapy-related cardiac dysfunction: time to recognize a new entity. *J Clin Oncol.* 2005;23:2900–2902. [PubMed: 15860848]
6. Ewer MS and Ewer SM. Cardiotoxicity of anticancer treatments: what the cardiologist needs to know. *Nat Rev Cardiol.* 2010;7:564–575. [PubMed: 20842180]
7. Arteaga CL and Engelman JA. ERBB receptors: from oncogene discovery to basic science to mechanism-based cancer therapeutics. *Cancer Cell.* 2014;25:282–303. [PubMed: 24651011]
8. Slamon DJ, Leyland-Jones B, Shak S, Fuchs H, Paton V, Bajamonde A, Fleming T, Eiermann W, Wolter J, Pegram M, Baselga J and Norton L. Use of chemotherapy plus a monoclonal antibody against HER2 for metastatic breast cancer that overexpresses HER2. *N Engl J Med.* 2001;344:783–792. [PubMed: 11248153]

9. Cote GM, Sawyer DB and Chabner BA. ERBB2 inhibition and heart failure. *N Engl J Med*. 2012;367:2150–2153. [PubMed: 23190227]
10. Lee KF, Simon H, Chen H, Bates B, Hung MC and Hauser C. Requirement for neuregulin receptor erbB2 in neural and cardiac development. *Nature*. 1995;378:394–398. [PubMed: 7477377]
11. Crone SA, Zhao YY, Fan L, Gu Y, Minamisawa S, Liu Y, Peterson KL, Chen J, Kahn R, Condorelli G, Ross J, Jr., Chien KR and Lee KF. ErbB2 is essential in the prevention of dilated cardiomyopathy. *Nat Med*. 2002;8:459–465. [PubMed: 11984589]
12. Ozcelik C, Erdmann B, Pilz B, Wettschureck N, Britsch S, Hubner N, Chien KR, Birchmeier C and Garratt AN. Conditional mutation of the ErbB2 (HER2) receptor in cardiomyocytes leads to dilated cardiomyopathy. *Proc Natl Acad Sci U S A*. 2002;99:8880–8885. [PubMed: 12072561]
13. Sayed N, Liu C and Wu JC. Translation of human-induced pluripotent stem cells: from clinical trial in a dish to precision medicine. *J Am Coll Cardiol*. 2016;67:2161–2176. [PubMed: 27151349]
14. Chen IY, Matsa E and Wu JC. Induced pluripotent stem cells: at the heart of cardiovascular precision medicine. *Nat Rev Cardiol*. 2016;13:333–349. [PubMed: 27009425]
15. Sharma A, Marceau C, Hamaguchi R, BurrIDGE PW, Rajarajan K, Churko JM, Wu H, Sallam KI, Matsa E, Sturzu AC, Che Y, Ebert A, Diecke S, Liang P, Red-Horse K, Carette JE, Wu SM and Wu JC. Human induced pluripotent stem cell-derived cardiomyocytes as an in vitro model for coxsackievirus B3-induced myocarditis and antiviral drug screening platform. *Circ Res*. 2014;115:556–566. [PubMed: 25015077]
16. Belkaya S, Kontorovich AR, Byun M, Mulero-Navarro S, Bajolle F, Cobat A, Josowitz R, Itan Y, Quint R, Lorenzo L, Boucherit S, Stoven C, Di Filippo S, Abel L, Zhang SY, Bonnet D, Gelb BD and Casanova JL. Autosomal recessive cardiomyopathy presenting as acute myocarditis. *J Am Coll Cardiol*. 2017;69:1653–1665. [PubMed: 28359509]
17. BurrIDGE PW, Li YF, Matsa E, Wu H, Ong SG, Sharma A, Holmstrom A, Chang AC, Coronado MJ, Ebert AD, Knowles JW, Telli ML, Witteles RM, Blau HM, Bernstein D, Altman RB and Wu JC. Human induced pluripotent stem cell-derived cardiomyocytes recapitulate the predilection of breast cancer patients to doxorubicin-induced cardiotoxicity. *Nat Med*. 2016;22:547–556. [PubMed: 27089514]
18. Drawnel FM, Boccardo S, Prummer M, Delobel F, Graff A, Weber M, Gerard R, Badi L, Kam-Thong T, Bu L, Jiang X, Hoflack JC, Kiialainen A, Jeworutzki E, Aoyama N, Carlson C, Burcin M, Gromo G, Boehringer M, Stahlberg H, Hall BJ, Magnone MC, Kolaja K, Chien KR, Bailly J and Iacone R. Disease modeling and phenotypic drug screening for diabetic cardiomyopathy using human induced pluripotent stem cells. *Cell Rep*. 2014;9:810–821. [PubMed: 25437537]
19. Sharma A, BurrIDGE PW, McKeithan WL, Serrano R, Shukla P, Sayed N, Churko JM, Kitani T, Wu H, Holmstrom A, Matsa E, Zhang Y, Kumar A, Fan AC, Del Alamo JC, Wu SM, Moslehi JJ, Mercola M and Wu JC. High-throughput screening of tyrosine kinase inhibitor cardiotoxicity with human induced pluripotent stem cells. *Sci Transl Med*. 2017;9:eaaf2584. [PubMed: 28202772]
20. Churko JM, BurrIDGE PW and Wu JC. Generation of human iPSCs from human peripheral blood mononuclear cells using non-integrative Sendai virus in chemically defined conditions. *Methods Mol Biol*. 2013;1036:81–88. [PubMed: 23807788]
21. BurrIDGE PW, Matsa E, Shukla P, Lin ZC, Churko JM, Ebert AD, Lan F, Diecke S, Huber B, Mordwinkin NM, Plews JR, Abilez OJ, Cui B, Gold JD and Wu JC. Chemically defined generation of human cardiomyocytes. *Nat Methods*. 2014;11:855–860. [PubMed: 24930130]
22. Zhao YY, Sawyer DR, Baliga RR, Opel DJ, Han X, Marchionni MA and Kelly RA. Neuregulins promote survival and growth of cardiac myocytes. Persistence of ErbB2 and ErbB4 expression in neonatal and adult ventricular myocytes. *J Biol Chem*. 1998;273:10261–10269. [PubMed: 9553078]
23. Hayakawa T, Kunihiro T, Ando T, Kobayashi S, Matsui E, Yada H, Kanda Y, Kurokawa J and Furukawa T. Image-based evaluation of contraction-relaxation kinetics of human-induced pluripotent stem cell-derived cardiomyocytes: correlation and complementarity with extracellular electrophysiology. *J Mol Cell Cardiol*. 2014;77:178–191. [PubMed: 25257913]
24. Ma N, Zhang J, Itzhaki I, Zhang SL, Chen H, Haddad F, Kitani T, Wilson KD, Tian L, Shrestha R, Wu H, Lam CK, Sayed N and Wu JC. Determining the pathogenicity of a genomic variant of uncertain significance using CRISPR/Cas9 and human-induced pluripotent stem cells. *Circulation*. 2018;138:2666–2681. [PubMed: 29914921]

25. Rabinowitz JD and White E. Autophagy and metabolism. *Science* 2010;330:1344–8. [PubMed: 21127245]
26. Doenst T, Nguyen TD and Abel ED. Cardiac metabolism in heart failure: implications beyond ATP production. *Circ Res.* 2013;113:709–724. [PubMed: 23989714]
27. Steinberg GR and Kemp BE. AMPK in health and disease. *Physiol Rev.* 2009;89:1025–78. [PubMed: 19584320]
28. Merrill GF, Kurth EJ, Hardie DG and Winder WW. AICA riboside increases AMP-activated protein kinase, fatty acid oxidation, and glucose uptake in rat muscle. *Am J Physiol.* 1997;273:E1107–E1112. [PubMed: 9435525]
29. Kim J, Yang G, Kim Y, Kim J and Ha J. AMPK activators: mechanisms of action and physiological activities. *Exp Mol Med.* 2016;48:e224. [PubMed: 27034026]
30. Lemmens K, Doggen K and De Keulenaer GW. Role of neuregulin-1/ErbB signaling in cardiovascular physiology and disease: implications for therapy of heart failure. *Circulation.* 2007;116:954–960. [PubMed: 17709650]
31. Odiete O, Hill MF and Sawyer DB. Neuregulin in cardiovascular development and disease. *Circ Res.* 2012;111:1376–1385. [PubMed: 23104879]
32. Singh KK, Shukla PC, Quan A, Lovren F, Pan Y, Wolfstadt JI, Gupta M, Al-Omran M, Leong-Poi H, Teoh H and Verma S. Herceptin, a recombinant humanized anti-ERBB2 monoclonal antibody, induces cardiomyocyte death. *Biochem Biophys Res Commun.* 2011;411:421–426. [PubMed: 21749857]
33. Fedele C, Riccio G, Malara AE, D'Alessio G and De Lorenzo C. Mechanisms of cardiotoxicity associated with ErbB2 inhibitors. *Breast Cancer Res Treat.* 2012;134:595–602. [PubMed: 22674190]
34. Riccio G, Esposito G, Leoncini E, Contu R, Condorelli G, Chiariello M, Laccetti P, Hrelia S, D'Alessio G and De Lorenzo C. Cardiotoxic effects, or lack thereof, of anti-ErbB2 immunoagents. *Faseb J.* 2009;23:3171–3178. [PubMed: 19417081]
35. Grazette LP, Boecker W, Matsui T, Semigran M, Force TL, Hajjar RJ and Rosenzweig A. Inhibition of ErbB2 causes mitochondrial dysfunction in cardiomyocytes: implications for herceptin-induced cardiomyopathy. *J Am Coll Cardiol.* 2004;44:2231–2238. [PubMed: 15582322]
36. Gordon LI, Burke MA, Singh AT, Prachand S, Lieberman ED, Sun L, Naik TJ, Prasad SV and Ardehali H. Blockade of the erbB2 receptor induces cardiomyocyte death through mitochondrial and reactive oxygen species-dependent pathways. *J Biol Chem.* 2009;284:2080–2087. [PubMed: 19017630]
37. Mohan N, Shen Y, Endo Y, ElZarrad MK and Wu WJ. Trastuzumab, but not pertuzumab, dysregulates HER2 signaling to mediate inhibition of autophagy and increase in reactive oxygen species production in human cardiomyocytes. *Mol Cancer Ther.* 2016;15:1321–1331. [PubMed: 27197303]
38. Necela BM, Axenfeld BC, Serie DJ, Kachergus JM, Perez EA, Thompson EA and Norton N. The antineoplastic drug, trastuzumab, dysregulates metabolism in iPSC-derived cardiomyocytes. *Clin Transl Med.* 2017;6:5. [PubMed: 28101782]
39. Jia G, Hill MA and Sowers JR. Diabetic cardiomyopathy: an update of mechanisms contributing to this clinical entity. *Circ Res.* 2018;122:624–638. [PubMed: 29449364]
40. Matsa E, BurrIDGE PW, Yu KH, Ahrens JH, Termglinchan V, Wu H, Liu C, Shukla P, Sayed N, Churko JM, Shao N, Woo NA, Chao AS, Gold JD, Karakikes I, Snyder MP and Wu JC. Transcriptome profiling of patient-specific human iPSC-cardiomyocytes predicts individual drug safety and efficacy responses in vitro. *Cell Stem Cell.* 2016;19:311–325. [PubMed: 27545504]
41. Gulati G, Heck SL, Ree AH, Hoffmann P, Schulz-Menger J, Fagerland MW, Gravdehaug B, von Knobelsdorff-Brenkenhoff F, Bratland A, Storås TH, Hagve TA, Rosjo H, Steine K, Geisler J and Omland T. Prevention of cardiac dysfunction during adjuvant breast cancer therapy (PRADA): a 2 × 2 factorial, randomized, placebo-controlled, double-blind clinical trial of candesartan and metoprolol. *Eur Heart J.* 2016;37:1671–1680. [PubMed: 26903532]
42. Bosch X, Rovira M, Sitges M, Domenech A, Ortiz-Perez JT, de Caralt TM, Morales-Ruiz M, Perea RJ, Monzo M and Esteve J. Enalapril and carvedilol for preventing chemotherapy-induced left ventricular systolic dysfunction in patients with malignant hemopathies: the OVERCOME trial



(prevention of left Ventricular dysfunction with Enalapril and carvedilol in patients submitted to intensive Chemotherapy for the treatment of Malignant hemopathies). *J Am Coll Cardiol*. 2013;61:2355–2362. [PubMed: 23583763]

43. Pituskin E, Mackey JR, Koshman S, Jassal D, Pitz M, Haykowsky MJ, Pagano JJ, Chow K, Thompson RB, Vos LJ, Ghosh S, Oudit GY, Ezekowitz JA and Paterson DI. Multidisciplinary approach to novel therapies in cardio-oncology research (MANTICORE 101-Breast): a randomized trial for the prevention of trastuzumab-associated cardiotoxicity. *Journal of Clinical Oncology*. 2017;35:870–877. [PubMed: 27893331]
44. Wang B, Nie J, Wu L, Hu Y, Wen Z, Dong L, Zou MH, Chen C and Wang DW. AMPK $\alpha$ 2 protects against the development of heart failure by enhancing mitophagy via PINK1 phosphorylation. *Circ Res*. 2018;122:712–729. [PubMed: 29284690]
45. Sasaki H, Asanuma H, Fujita M, Takahama H, Wakeno M, Ito S, Ogai A, Asakura M, Kim J, Minamino T, Takashima S, Sanada S, Sugimachi M, Komamura K, Mochizuki N and Kitakaze M. Metformin prevents progression of heart failure in dogs: role of AMP-activated protein kinase. *Circulation*. 2009;119:2568–2577. [PubMed: 19414638]
46. Yin M, van der Horst IC, van Melle JP, Qian C, van Gilst WH, Sillje HH and de Boer RA. Metformin improves cardiac function in a nondiabetic rat model of post-MI heart failure. *Am J Physiol Heart Circ Physiol*. 2011;301:H459–H468. [PubMed: 21572014]
47. Gundewar S, Calvert JW, Jha S, Toedt-Pingel I, Ji SY, Nunez D, Ramachandran A, Anaya-Cisneros M, Tian R and Lefer DJ. Activation of AMP-activated protein kinase by metformin improves left ventricular function and survival in heart failure. *Circ Res*. 2009;104:403–411. [PubMed: 19096023]
48. Lexis CP, van der Horst IC, Lipsic E, Wieringa WG, de Boer RA, van den Heuvel AF, van der Werf HW, Schurer RA, Pundziute G, Tan ES, Nieuwland W, Willemsen HM, Dorhout B, Molmans BH, van der Horst-Schrivers AN, Wolffenbuttel BH, ter Horst GJ, van Rossum AC, Tijssen JG, Hillege HL, de Smet BJ, van der Harst P, van Veldhuisen DJ and Investigators G-I. Effect of metformin on left ventricular function after acute myocardial infarction in patients without diabetes: the GIPS-III randomized clinical trial. *JAMA*. 2014;311:1526–1535. [PubMed: 24687169]
49. Hesén NA, Riksen NP, Aalders B, Ritskes-Hoitinga M, El Messaoudi S and Wever KE. A systematic review and meta-analysis of the protective effects of metformin in experimental myocardial infarction. *PLoS One*. 2017;12:e0183664. [PubMed: 28832637]
50. Alers S, Löffler AS, Wesselborg S and Stork B. Role of AMPK-mTOR-Ulk1/2 in the regulation of autophagy: cross talk, shortcuts, and feedbacks. *Mol Cell Biol*. 2012;32:2–11. [PubMed: 22025673]

## CLINICAL PERSPECTIVE

### What is new?

- We show that human induced pluripotent stem cell-derived cardiomyocytes (iPSC-CMs) can recapitulate key features of trastuzumab-induced cardiac dysfunction in patients using 10 different iPSC lines, including from patients with trastuzumab therapy.
- We found that alterations in the cardiac energy metabolism pathways play an important role in cardiomyocyte dysfunction following trastuzumab treatment.

### What are the clinical implications?

- Patient-specific iPSC-CMs can be used as a platform to assess individual risks for cardiac dysfunction during trastuzumab therapy.
- Trastuzumab-induced cardiac dysfunction in human iPSC-CMs can be ameliorated by AMPK activators, suggesting that these drugs could be repurposed for the treatment of this cardiac dysfunction.

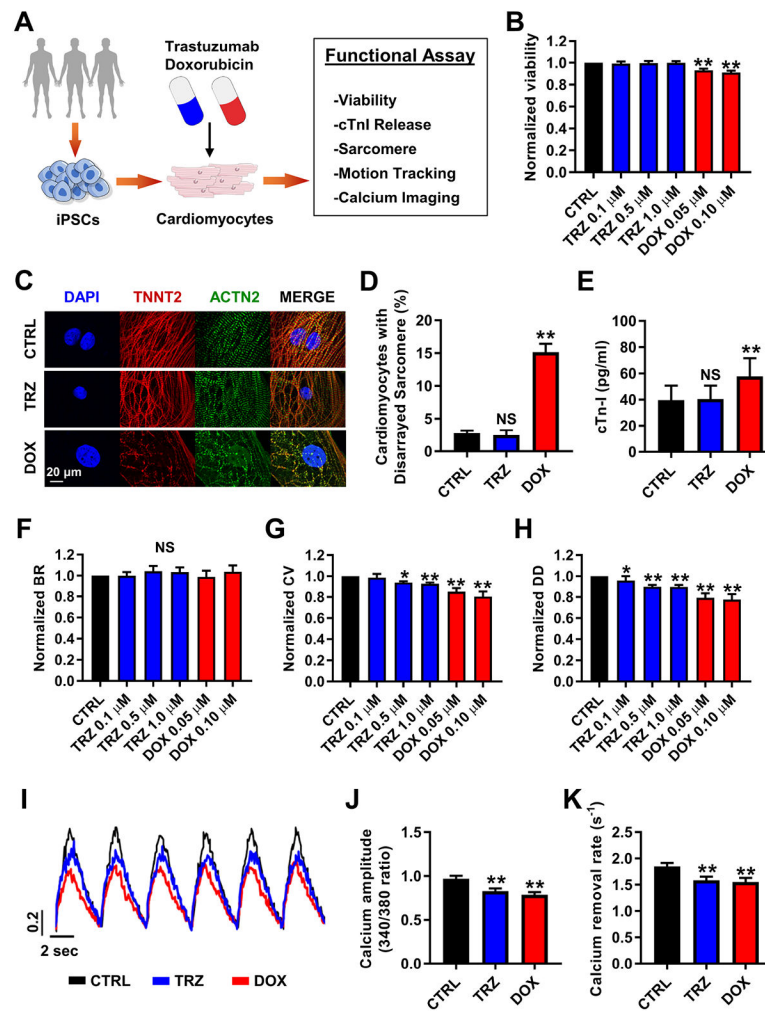


**Figure 1. Recapitulating the clinical phenotype of trastuzumab-induced cardiac dysfunction with iPSC-CMs.**

(A) Schematic outline of study workflow. Human iPSC lines were generated from three healthy individuals. After cardiac differentiation, beating iPSC-CMs were exposed to trastuzumab or doxorubicin for 7 days and used for subsequent functional analysis. (B) Quantification of cell viability after 7 days of drug treatment in control (CTRL, black), trastuzumab (TRZ, blue) (0.1–1.0  $\mu$ M), or doxorubicin (DOX, red) (in 0.05 and 0.10  $\mu$ M). Cell viability was not affected by trastuzumab but was significantly reduced by doxorubicin. Data were obtained using iPSC-CMs from three individuals and the assay was repeated three times. (C) Representative images of immunostaining of iPSC-CMs with cardiac troponin T (TNNT2) and alpha-actinin (ACTN2) after 7 days of drug treatment. Sarcomere disarray was induced by doxorubicin in iPSC-CMs, but not by trastuzumab. Scale bar, 20  $\mu$ m. (D) Percentages of iPSC-CMs with disarrayed sarcomere assessed by immunostaining. Data were obtained using iPSC-CMs from three individuals and 40–60 cells were analyzed per each line for each condition. (E) Quantification of cardiac troponin I in the culture medium. Cardiac troponin I release was increased by doxorubicin, but not by trastuzumab. Data were obtained using iPSC-CMs from three individuals and the assay was repeated twice. (F–H) Contractile properties in iPSC-CMs were quantified by video microscopy-based motion

vector analysis after 7 days of drug treatment. Spontaneous beating rate (F) was not affected by drug treatment. Trastuzumab reduced contraction velocity (G) and deformation distance (H) in iPSC-CMs similar to doxorubicin. Data were obtained using iPSC-CMs from three individuals and the assay was repeated three times. **(I-K)** Calcium imaging of iPSC-CMs conducted after 7 days of drug treatment. Representative recording of calcium activity (I) and quantification of calcium imaging parameters in iPSC-CMs. Trastuzumab reduced systolic calcium amplitude (J) and diastolic calcium removal (K), similar to doxorubicin. Data were obtained using iPSC-CMs from three individuals and 30–40 cells were analyzed per each line for each condition. All data are expressed as means  $\pm$  SEM. Statistical analyses were performed using one-way ANOVA followed by the Holm–Sidak multiple comparisons test. NS, not significant; \*,  $P < 0.05$ ; \*\*,  $P < 0.01$ , compared with control group.

Author Manuscript

Author Manuscript

Author Manuscript

Author Manuscript

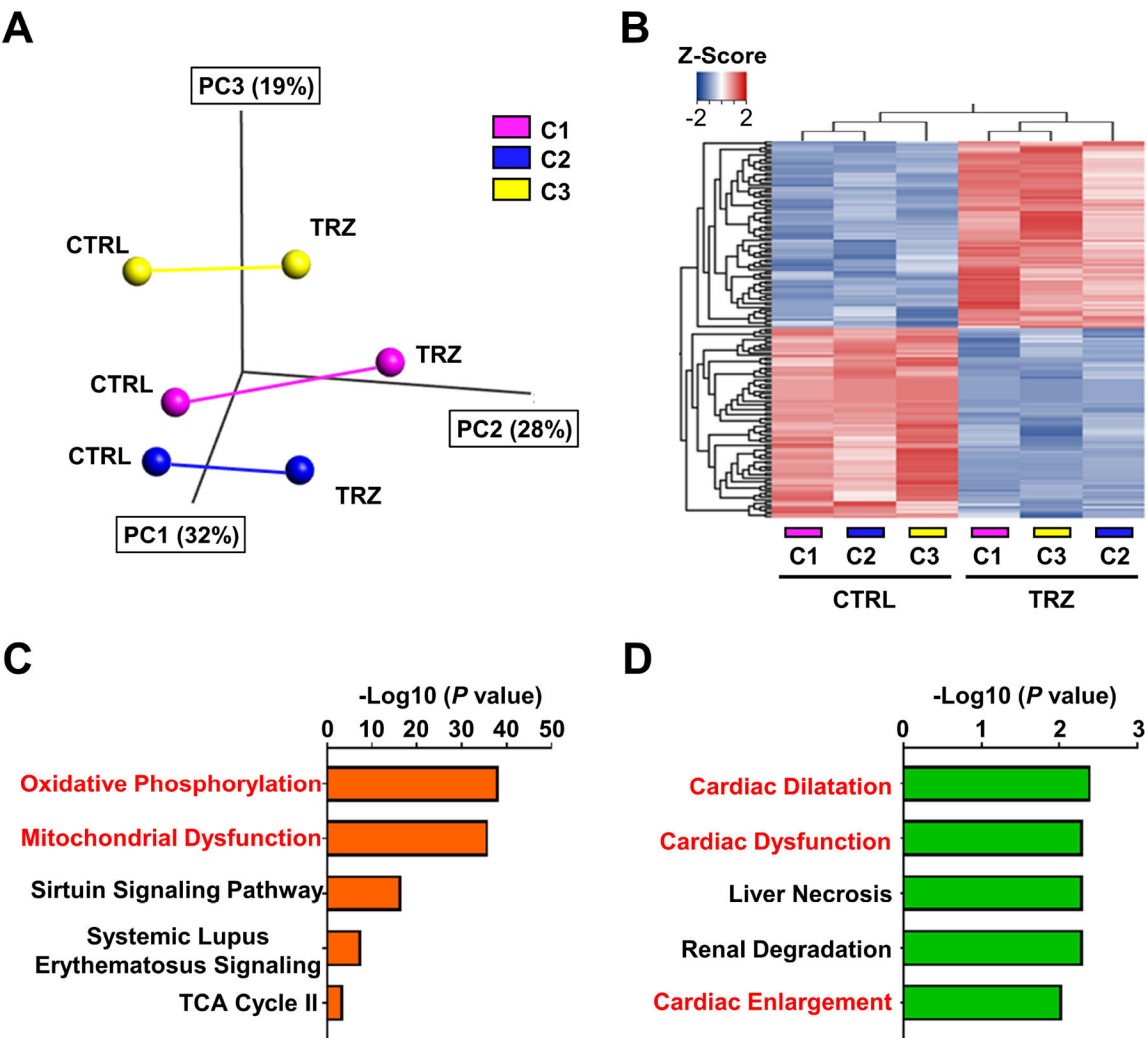


**Figure 2. Transcriptomic analysis of the effect of trastuzumab in human iPSC-CMs.** (A-B) Three-dimensional principal component analysis (PCA) plot of all expressed genes (A) and hierarchical clustering of genes with false discovery rate (FDR) < 0.1 and fold-change > 1.5 (B) of RNA-seq data from iPSC-CMs of 3 individuals treated with trastuzumab (TRZ) or untreated control groups (CTRL), showing individual variation and the response to trastuzumab treatment in transcriptome. *Pink*: control line 1 (C1), *Blue*: control line 2 (C2), *Yellow*: control line 3 (C3). (C-D) Ingenuity pathway analysis (IPA) of altered expressed genes identified by RNA-seq revealed top five canonical pathways (C) and top five toxicity functions (D) related to trastuzumab treatment in iPSC-CMs.

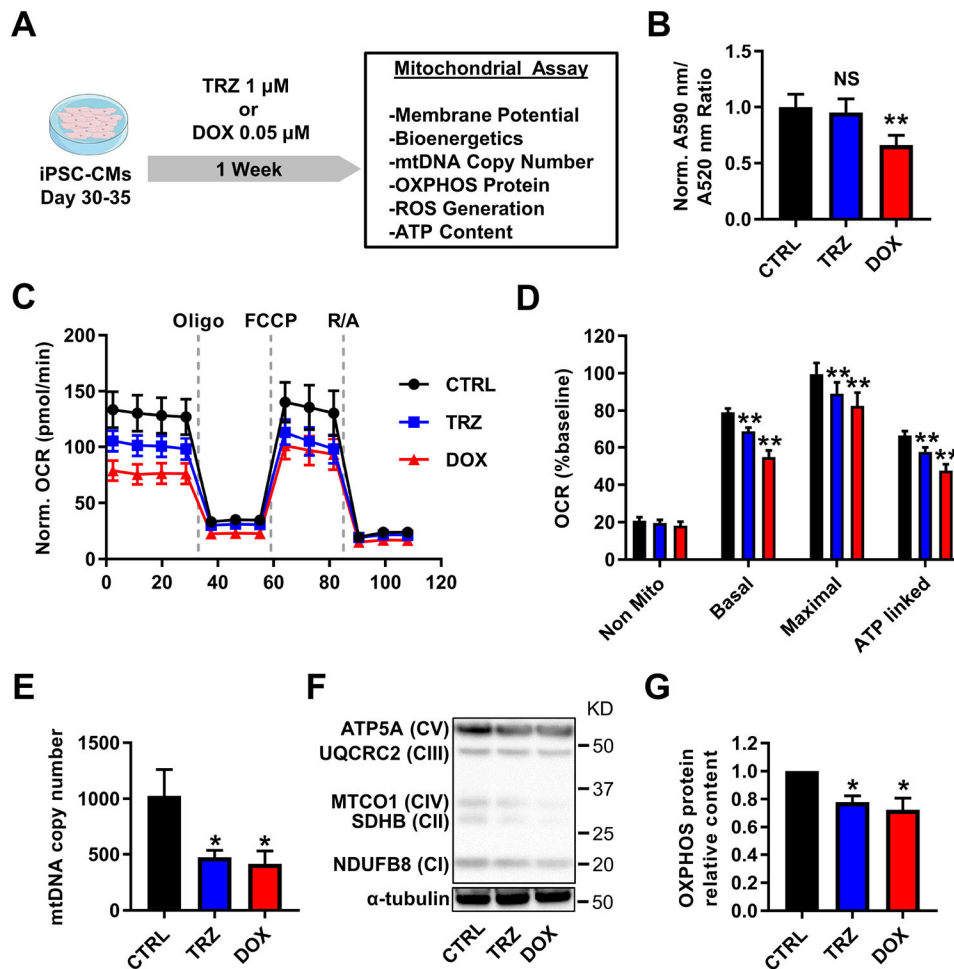


**Figure 3. Assessment of the effect of trastuzumab on mitochondrial function in human iPSC-CMs.**

(A) Schematic workflow of the experimental design. (B) Mitochondrial membrane potential in iPSC-CMs was measured using the JC10 dye after 7 days of drug treatment in control (CTRL, black), trastuzumab (TRZ, blue), or doxorubicin (DOX, red). (C-D) Oxygen-consumption rate (OCR) was measured in iPSC-CMs following trastuzumab or doxorubicin treatment by a mitochondrial stress test using the Seahorse XF96 extracellular-flux analyzer. (C) Representative plot of OCR measured in iPSC-CMs following the drug treatment. Sequential addition of oligomycin, FCCP, and rotenone + antimycin (R/A) is indicated in the graph. (D) Quantification and statistical analysis of Seahorse extracellular-flux assay results. (E) Quantification of mtDNA copy number in iPSC-CMs following the drug treatment. (F-G) Effect of drugs on mitochondrial respiratory complexes protein in iPSC-CMs. Representative image of Western blot analysis for five mitochondrial oxidative phosphorylation complex proteins (NDUFB8 for complex I; SDHB for complex II; UQCRC2 for complex III; MTCO1 for complex IV; ATP5A for complex V) (F), and quantification of the total band densities for all five proteins normalized with the corresponding  $\alpha$ -tubulin (G). Data were obtained using iPSC-CMs from three individuals, and the assays were repeated twice for mitochondrial stress test and Western blot analysis, or three times for other assays. All data are expressed as means  $\pm$  SEM. Statistical analyses



were performed using one-way ANOVA followed by the Holm–Sidak multiple comparisons test. NS, not significant; \*,  $P < 0.05$ ; \*\*,  $P < 0.01$ , compared with control group.

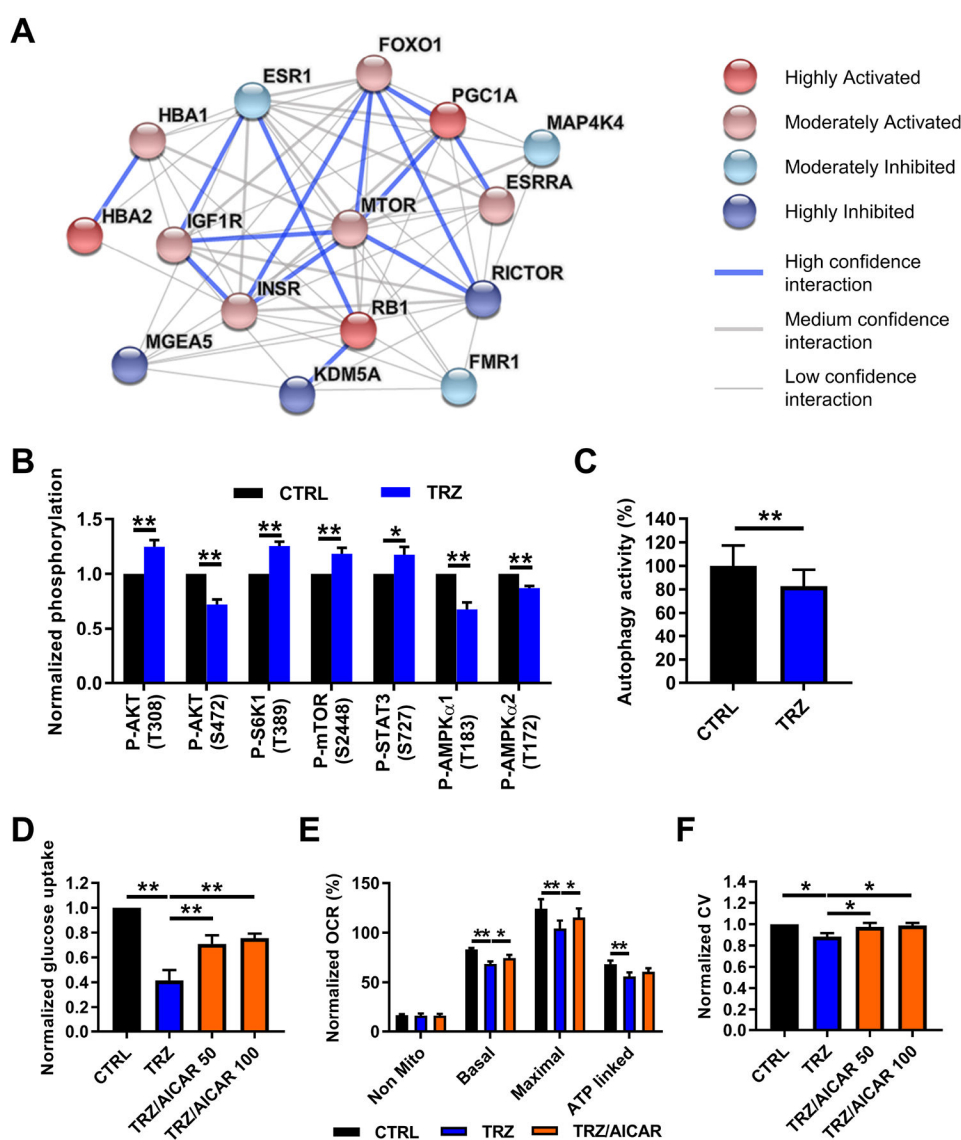


**Figure 4. Changes in energy metabolism pathway in human iPSC-CMs induced by trastuzumab.** (A) STRING network analysis of the upstream regulators revealing alteration of key genes regulating cardiac energy metabolism after trastuzumab treatment. (B) Phosphorylation array on iPSC-CMs after trastuzumab treatment demonstrates changes in kinase activities, consistent with results from the upstream analysis. (C) Quantification of autophagy level in iPSC-CMs after trastuzumab treatment by Cyto-ID staining. (D) Quantification of glucose uptake in iPSC-CMs after trastuzumab treatment with or without the co-treatment of AICAR (50 or 100  $\mu$ M). (E) OCR measured using the mitochondrial stress test in iPSC-CMs after trastuzumab treatment with or without the co-treatment of 100  $\mu$ M AICAR. (F) Contraction velocity quantified by video microscopy-based motion vector analysis in iPSC-CMs after trastuzumab treatment with or without the co-treatment of AICAR (50 or 100  $\mu$ M). In each bar graph, the *black* bars indicate the control (CTRL); *blue* bars, trastuzumab (TRZ); and *orange* bars, trastuzumab with AICAR (TRZ/AICAR). Data were obtained using iPSC-CMs from three individuals, and the assays were repeated four times for autophagy detection and

phosphorylation array, or three times for other assays. All data are expressed as means  $\pm$  SEM. Statistical analyses were performed using the two-tailed Student's t-test (Fig. B-C), or one-way ANOVA followed by the Holm–Sidak multiple comparisons test (Fig. D-F). \*,  $P < 0.05$ ; \*\*,  $P < 0.01$ .

Author Manuscript

Author Manuscript

Author Manuscript

Author Manuscript

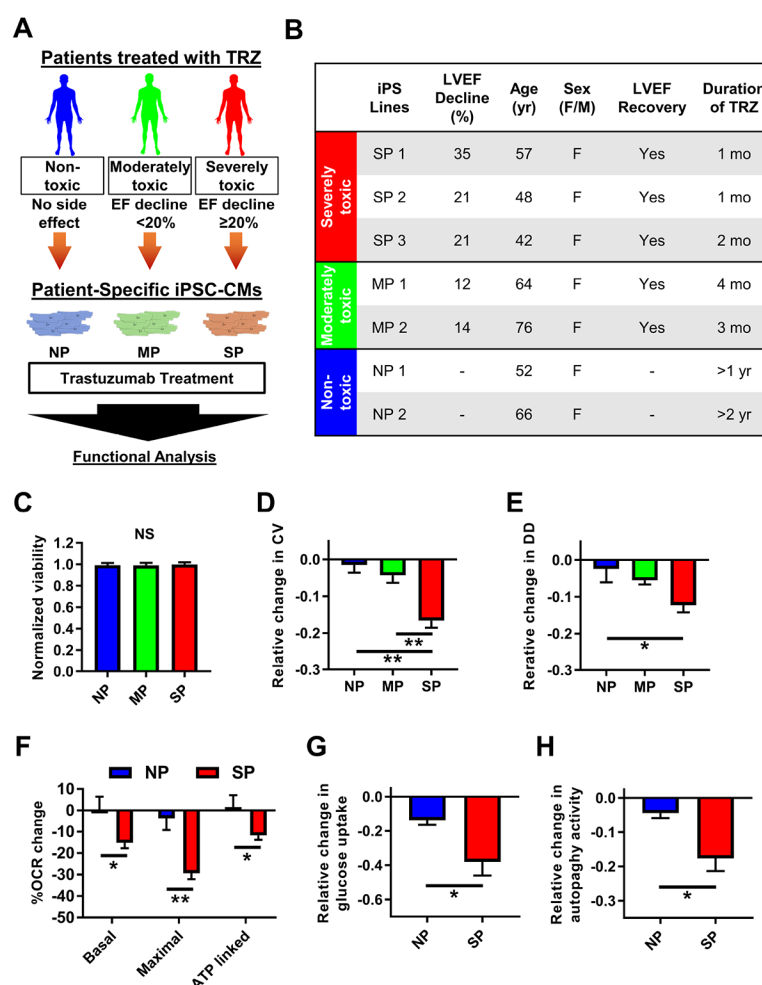


**Figure 5. Assessing the effect of trastuzumab in patient-specific iPSC-CMs.**

(A) Schematic illustrating the experimental workflow. Patient-specific iPSC-CMs were generated from seven breast cancer patients receiving trastuzumab therapy. Two patients did not exhibit cardiac dysfunction (NP, *blue*), two patients experienced moderate LVEF decline (MP, *green*), and three patients experienced severe LVEF decline (SP, *red*). Substantial LVEF decline is defined as a decrease in LVEF of > 10% but < 20% (moderate), or ≥ 20% (severe) from baseline to less than 55%. Patient-specific iPSC-CMs were then subjected to functional analysis following trastuzumab treatment. (B) Patient characteristics recruited for this study. Age, at time of consent; LVEF, left ventricular ejection fraction; LVEF recovery, improvement of LVEF after trastuzumab withdrawal; duration of TRZ, the duration from initiation to discontinuation of trastuzumab therapy due to LVEF decline; mo, months; yr, years. (C) Cell viability in iPSC-CMs after trastuzumab treatment. (D-E) Changes in contractile properties in iPSC-CMs after trastuzumab treatment. Trastuzumab treatment significantly impaired contraction velocity (D) and deformation distance (E) of iPSC-CMs to a greater extent in SP group, compared to NP or MP group. (F) Oxygen consumption rate (OCR) changes under mitochondrial stress in iPSC-CMs after trastuzumab treatment. *Blue*: NP lines, *Red*: SP lines. (G) Changes in glucose uptake in iPSC-CMs after trastuzumab treatment. (H) Changes in autophagy level in iPSC-CMs after trastuzumab treatment. Data

were obtained by using iPSC-CMs from all patients to assess cell viability and contractile properties or by using iPSC-CMs from all lines in SP and NP group for the other assays, and all assays were repeated three times for each line. All data are expressed as means  $\pm$  SEM. Statistical analyses were performed using one-way ANOVA followed by the Holm–Sidak multiple comparisons test (Fig. C-E), or the two-tailed Student's t-test (Fig. F-H). \*,  $P < 0.05$ ; \*\*,  $P < 0.01$ .

Author Manuscript

Author Manuscript

Author Manuscript

Author Manuscript

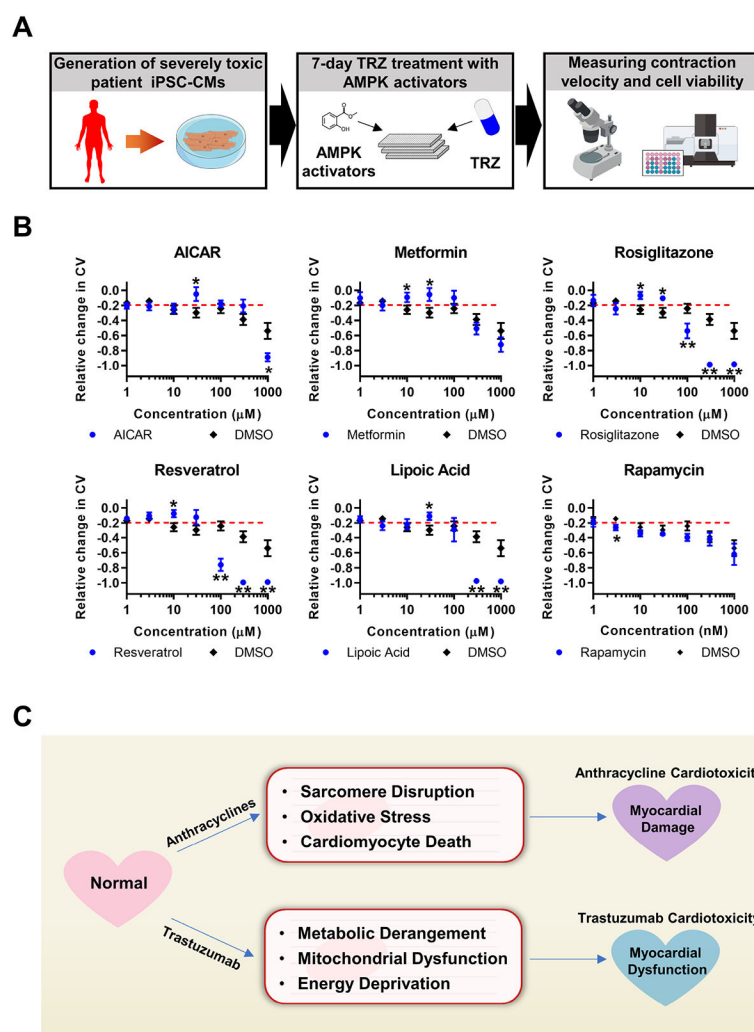


**Figure 6. Drug testing for trastuzumab-induced cardiac dysfunction using patient-specific iPSC-CMs.**

(A) Schematic illustrating the experimental workflow. Human iPSC-CMs generated from the severely toxic patient (SP1 iPSC-CMs) were subjected to drug testing. (B) Changes in contraction velocity in SP1 iPSC-CMs after trastuzumab treatment with co-treatment of AMPK activators and rapamycin. The red dotted line indicates the value in SP1 iPSC-CMs treated only with trastuzumab. The assay was repeated nine times. All data are expressed as means  $\pm$  SEM. Statistical analyses were performed using the two-tailed Student's t-test. \*,  $P < 0.05$ ; \*\*,  $P < 0.01$ , compared with vehicle control treated with same volume of DMSO.

(C) Pathogenesis of chemotherapy-induced cardiotoxicity. Two different types of chemotherapy-induced cardiotoxicity can be explained by the presence of different underlying molecular aberrations in cardiomyocytes following cancer therapy. Targeting the altered energy metabolism may work as a potential therapeutic approach for cardiotoxicity induced by trastuzumab.